

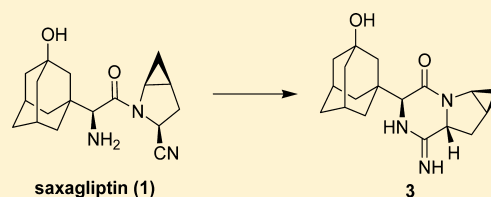
Kinetic and Mechanistic Insight into the Thermodynamic Degradation of Saxagliptin

G. Scott Jones,* Scott A. Savage, Sabrina Ivy, Patrick L. Benitez,[†] and Antonio Ramirez

Chemical Development, Bristol–Myers Squibb Company, One Squibb Drive, New Brunswick, New Jersey 08903, United States

S Supporting Information

ABSTRACT: The dipeptidyl peptidase-IV inhibitor saxagliptin (Onglyza) can undergo a thermodynamically favored cyclization to form the corresponding cyclic amidine. The kinetics and mechanism of this conversion were examined to develop a commercial synthesis that afforded saxagliptin with only trace levels of this key byproduct. Important findings of this work are the identification of a profound solvent effect and the determination of an autocatalytic pathway. Both of these phenomena result from transition structures involving proton transfer.



Dipeptidyl peptidase-IV (DPP-IV) inhibitors are an important new class of oral hyperglycemic medications. 2-Cyano pyrrolidine derivatives such as saxagliptin¹ (**1**) have been studied extensively for activity as DPP-IV inhibitors because of the enzyme's specificity for substrates with an amino-terminal proline. However, many members of this chemotype suffer from chemical instability, rendering them impractical for drug development because of an inherent inability to be synthesized or formulated at the scales required for commercial pharmaceutical manufacturing.² As demonstrated in Scheme 1, these compounds are prone to undergo cyclization, whereby the N-terminal amine attacks the nitrile, forming inactive cyclic amidines or their diketopiperazine hydrolysis products.

In the case of saxagliptin, substantially increased stability was designed into the molecule via side-chain bulk with an adamantyl group as well as by addition of the methano-bridge on the proline moiety.³ Although these structural modifications address the cyclization issue effectively from a physiological perspective,⁴ minimizing the formation of the cyclic amidine **3** impurity remained the primary challenge of designing a process to synthesize pure **1** on a commercial manufacturing scale.⁵ This paper discusses the roles of protic solvents and autocatalysis in the cyclization of **1** to **3** and the related development of a kinetic model that was utilized to guide process development.

The cyclization reactions were monitored by HPLC analysis of reaction streams, and the concentration of species **1**, **3**, and **4** was determined by direct comparison to fully characterized samples prepared independently. Unless otherwise noted, all experiments utilized pure **1**, containing <0.1% of amidine **3** and no diketopiperazine **4**. As saxagliptin is isolated as the crystalline monohydrate,⁵ a molar equivalent of water was present in all solutions, and thus the relatively slow hydrolysis of **3** to **4** was observed during reactions. The reported rate constants and activation energies were regressed from the concentration profiles of species **1**, **3**, and **4** using the commercially available software, DynoChem.

With regards to cyclic amidines **2** and **3**, it is worth noting that standard solution reaction conditions afford exclusively epimer **3**. The body of evidence supports Scheme 1, namely, that rate-limiting cyclization occurs first, followed by rapid epimerization. First, monitoring the reaction in the solid state, where the rate of epimerization of **2** is reduced, revealed the transient presence of intermediate **2**, which subsequently converted to epimer **3**.⁶ Second, the nitrile epimer of **1** was observed to cyclize to **3** at a rate that was indistinguishable from the rate of saxagliptin (**1**) cyclization.⁷ Finally, the proton alpha to the amidine in **3** readily exchanges with deuterium in D₂O solutions, whereas a similar exchange does not occur at this position for solutions of saxagliptin (**1**) in D₂O. Together, these data support the proposed mechanism in Scheme 1 and serve as evidence against an alternative mechanism, in which rate-limiting epimerization of saxagliptin (**1**) is followed by rapid cyclization to amidine **3**. The hydrolysis of amidine **3** to diketopiperazine **4** occurs in the presence of water and is not critical to understanding the mechanism and kinetics of the cyclization but is presented here for completeness.

The initial rates for the formation of **3** were monitored in the process solvents isopropanol (*i*-PrOH), dichloromethane, and ethyl acetate at 40 °C and [1] = 0.04 M. Under these conditions, the cyclization displays a clean first-order dependence on saxagliptin concentration. The studies showed that the cyclizations in *i*-PrOH were 5-fold faster than the cyclizations in ethyl acetate and 3-fold faster when compared to dichloromethane. Further examination revealed that the rates correlated well with the solvent's propensity to participate in proton transfer reactions, namely, (a) the solvent's p*K*_s, where *K*_s is the autoprotolysis equilibrium constant of the protic or protogenic solvent, and (b) the solvent's proton affinity, which represents the solvent's absolute gas phase basicity (Figure 1).⁸

Received: October 3, 2011

Published: November 4, 2011

Scheme 1. Undesirable Conversion of Saxagliptin to Amidine and Diketopiperazine Byproducts

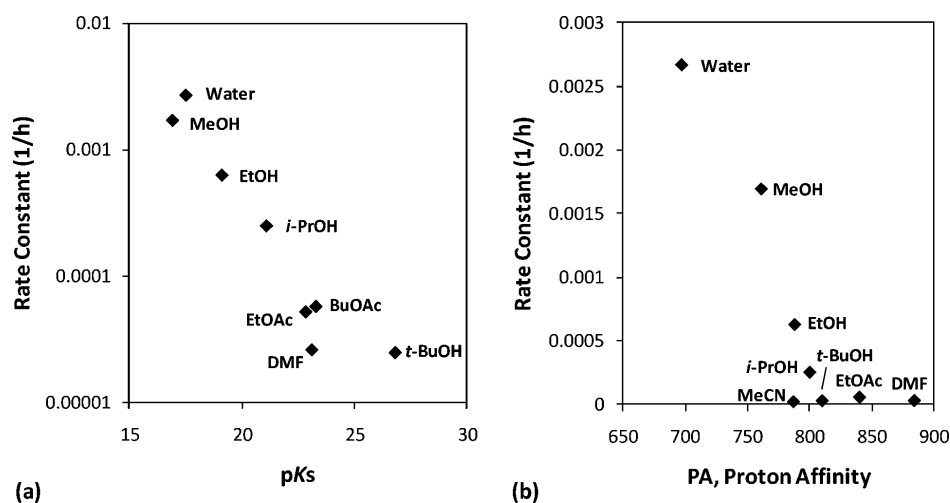
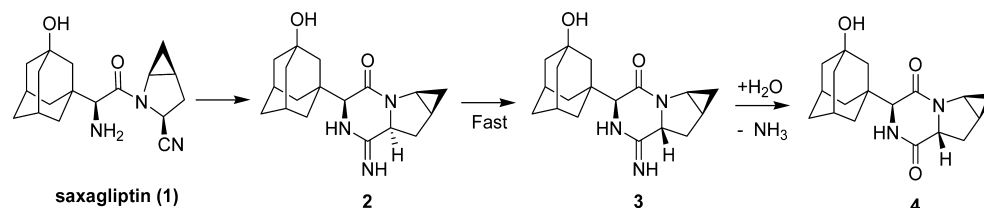


Figure 1. Measured rate constant versus solvent's (a) pK_s , where K_s is the autoprotolysis equilibrium constant of the protic or protogenic solvent and (b) proton affinity.

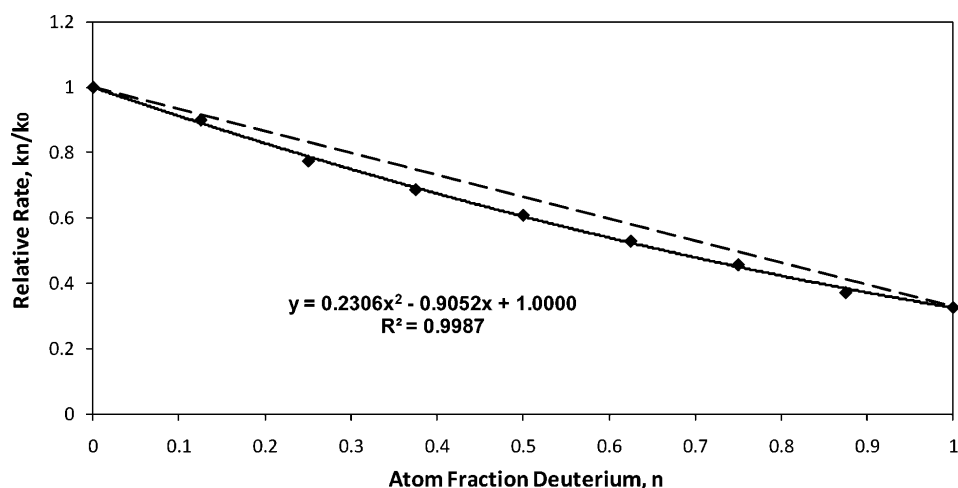


Figure 2. Plot of relative rate versus deuterium atom fraction.

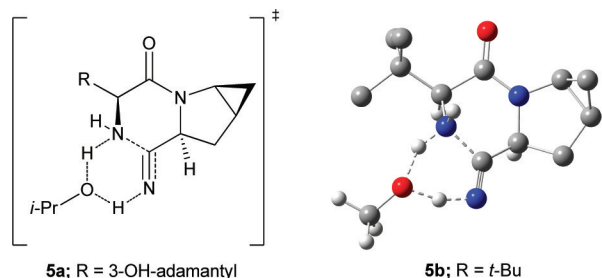
To ascertain the participation of *i*-PrOH in the reaction coordinate and its role in the manufacturing process, we carried out proton inventory studies by monitoring the kinetic isotope effect, k_n/k_0 , as a function of the mole fraction of *i*-PrOH, n , at 40 °C and $[1] = 0.04$ M. The Gross–Butler equation was employed for purposes of evaluating the results (eq 1).⁹ The polynomial fit of the experimental data to a derived form of eq 1¹⁰ (Figure 2) reveals a number of insights about the reaction of interest. First, a normal kinetic isotope effect $k_H/k_D \sim 3$ indicates that a proton transfer involving *i*-PrOH is indeed rate limiting. Second, the curvature of the line that fits the data (solid line in Figure 2) provides insight into the number of protons involved in the transition state.^{9,11} If only a proton from the amine group in **1** was transferred in the

transition state, the rates would vary linearly with deuterium content (dashed line in Figure 2). The fact that the data are best fit with a quadratic implies that two protons are moving in the transition state. Solving the quadratic equation that best fits the data in Figure 2 gives two fractionation factors $\Phi_1^{TS} \sim \Phi_2^{TS} \sim 0.55$. The Φ_i^{TS} values and the overall kinetic isotope effect reported here are in line with proton inventories reported by others for two simultaneous proton transfers.^{9,11}

$$\frac{k_n}{k_0} = \frac{\prod_{i=1}^{n_{TS}} (1 - n + n\Phi_i^{TS})}{\prod_{i=1}^{n_R} (1 - n + n\Phi_i^R)} \quad (1)$$

The simplest and most general transition state that is consistent with the experimental observations is transition

structure **5a**. A search for transition structures with DFT calculations at the B3LYP/6-31+G(d)/PCM¹² level using MeOH instead of *i*-PrOH and a model substrate ($R = t\text{-Bu}$) for simplification afforded structure **5b**, which displays a double proton transfer between the alcohol solvent and the 2-cyano pyrrolidine with concomitant N–CN bond formation. The calculations overestimate the ΔG_{298}^\ddagger value for **5b** (149 kJ/mol) relative to the experimental results shown in Table 2 but are in qualitative agreement with the higher stabilization imparted by the autocatalytic pathway (*vide infra*).¹³

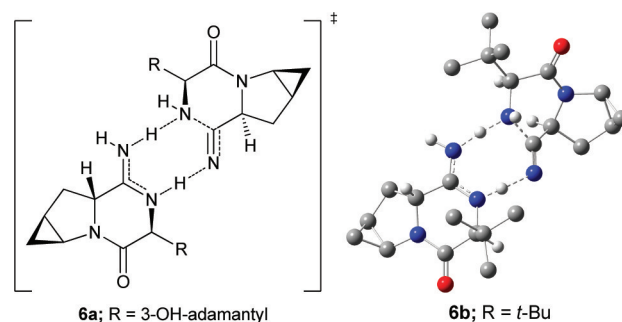


Interestingly, monitoring the formation of **3** at higher temperatures and concentrations of **1** in *i*-PrOH (i.e., 75 °C and $[1] = 0.85\text{ M}$) afforded a sigmoidal profile instead of the exponential shape expected for a first-order dependence in substrate. The sigmoidal profile suggested the existence of autocatalysis, which was supported by kinetic modeling demonstrating that the best fit required an autocatalytic component in amidine **3** (Figure 3a). The simple three-reaction model is shown in Table 1. At the maximum concentration of amidine **3**, the rate of the autocatalytic pathway is approximately 20-fold greater than the unimolecular conversion of **1** to **3**. To further support the autocatalysis hypothesis, a series of reactions was conducted, in which increasing amounts of cyclic amidine **3** were spiked into a 0.375 M solution of **1** in *i*-PrOH at 75 °C. Analysis of the initial rates from these reactions confirmed that the cyclization rates are directly proportional to the initial concentrations of amidine **3** (Figure 3b). Taken together, these data unequivocally demonstrate autocatalysis as a key factor in the decomposition of **1** at high concentrations and temperatures.

Table 1. Rate Equations Corresponding to Figure 3a

reaction	rate expression	rate constant
$1 \rightarrow 3$	$k [1]$	0.002 1/h
$1 + 3 \rightarrow 3 + 3$	$k [1] [3]$	0.158 L/mol-h
$3 + \text{H}_2\text{O} \rightarrow 4 + \text{NH}_3$	$k [3] [\text{H}_2\text{O}]$	0.068 L/mol-h

Two hypotheses were considered as possible explanations for the autocatalysis. First, a simple change in the concentration of basic species during the reaction might be responsible for the increasing rates of cyclization.¹⁴ Alternatively, amidine **3** could promote a double proton transfer transition state such as **6a** analogous to transition state **5a**. Similar complexes have been proposed in the 2-pyridone catalyzed mutarotation of tetramethyl glucose,¹⁵ the lactim–lactam tautomerism of 2-pyridone,¹⁶ and the reactions of various amidines.¹⁷



To investigate the two scenarios, we examined the effect of additives morpholine (**7**) and 2-aminothiazoline (**8**) upon the cyclization rates. The $\text{p}K_a$ values for the conjugated acids of **7** and **8**, 8.3 and 8.7 respectively, are similar to that of amidine **3** (8.3),¹⁸ but **7** and **8** differ in their capacity to mediate proton transfer-based transition states akin to **6a**. Interestingly, addition of 0.1 equiv morpholine (**7**) resulted in rates comparable to those measured in the absence of additive, whereas addition of 0.1 equiv 2-amino-2-thiazoline (**8**) afforded faster rates that reproduced those measured in the presence of 0.1 equiv amidine **3** (Figure 4). The excellent agreement between the amidine- and thiazoline-spiked experiments and the absence of any effect in the morpholine-spiked reaction

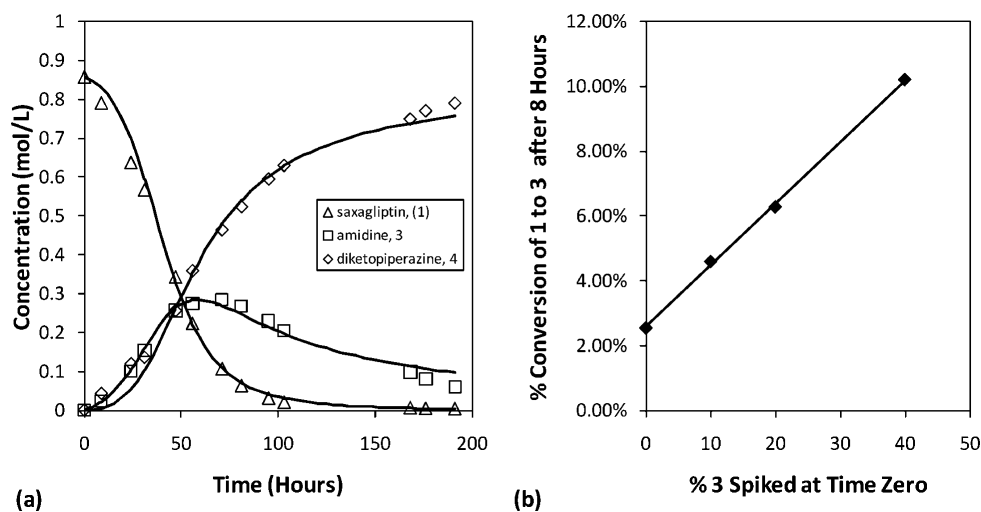


Figure 3. (a) Representative concentration profiles for the cyclization of saxagliptin ($[1] = 0.85\text{ M}$ in *i*-PrOH at 75 °C). (b) Plot of initial cyclization rates versus concentration of amidine **3** ($[1] = 0.375\text{ M}$ in *i*-PrOH at 75 °C).

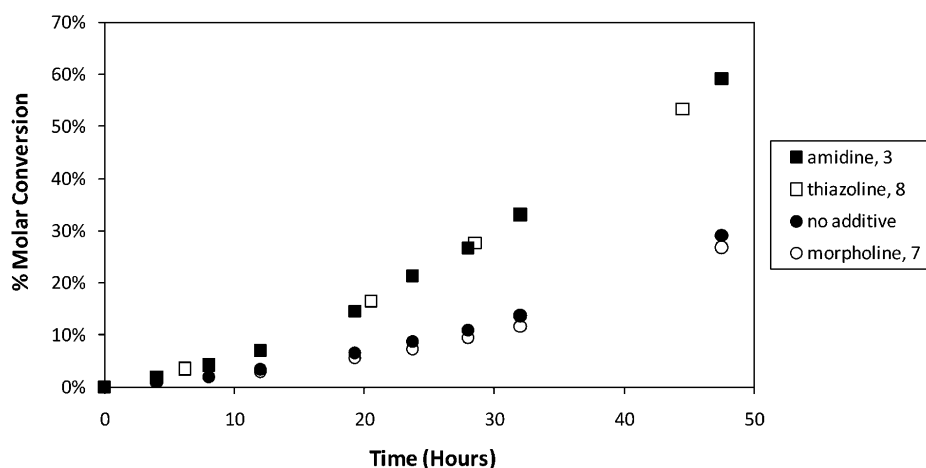


Figure 4. Molar conversion versus time for spiking experiments comparing additives: amidine **3**, thiazoline **8**, morpholine **7**, with a control experiment with no additive.

support the participation of the amidine functionality as proposed in transition structure **6a**. A simplified transition structure **6b** ($R = t\text{-Bu}$) could be located using DFT computations at the B3LYP/6-31G+(d)/PCM level.¹² **6b** displays a double proton transfer between the 2-cyano pyrrolidine and the amidine with simultaneous formation of the incipient N–CN bond. The calculations predict a ΔG_{298}^\ddagger value of 96 kJ/mol for the autocatalytic transition state **6b**, which is fairly close to the experimental estimate of 82 kJ/mol presented in the following section.



The goal of this work was to improve our ability to control the undesired formation of **3** during the synthesis of saxagliptin. It is worth noting that even in *i*-PrOH, the rate of the undesired conversion is rather slow. However, within the context of the long processing times encountered in commercial manufacturing and the stringent purity requirements of an active pharmaceutical ingredient, even such relatively slow conversions require detailed understanding. The cyclization kinetic studies represent ideal systems, using very pure starting materials and single-solvent reaction matrices that did not change in time. Despite the fact that these conditions are somewhat removed from those encountered in the commercial manufacturing process, the knowledge gained in these studies formed the foundation of a kinetic model for the commercial process.

In the commercial process, the unit operation that required the greatest understanding to minimize the cyclization was the distillation, or concentration, that took place following the formation of **1**. This operation was of particular interest because a number of parameters with potential to influence cyclization kinetics (i.e., temperature, solvent composition, and concentration) change in time as the operation proceeds. A set of experiments was undertaken to determine the influence of these parameters on the rate of cyclization during the concentration. Samples of the processing stream were taken at the beginning, middle, and end of the concentration, representing discrete conditions encountered in the manufacturing process. Each stream was further subdivided and held at different temperatures in order to monitor the cyclization rate

and obtain activation energies from the rate constants.¹⁹ The experimental data across these conditions and in time were well represented by the two simple rate expressions shown in Table

Table 2. Rate Equations Corresponding to Figure 5

rate expression	E_a (kJ/mol)	ΔG_{298}^\ddagger (kJ/mol)
$k [1] [i\text{-PrOH}]$	60	98
$k [1] [3]$	49	82

2. Consistent with transition states **5** and **6**, both rate expressions involve bimolecular interactions between **1** and *i*-PrOH²⁰ or between **1** and **3**, respectively. As demonstrated by the parity plot shown in Figure 5, the simple model based on the mechanistic studies described here does an excellent job of predicting reaction performance in the commercial manufacturing process.

In summary, amidine **3** was the key impurity that required control during process development of the DPP-IV inhibitor saxagliptin. Amidine **3** is formed by a cyclization of saxagliptin that involves a double proton transfer. Hydrogen bonding and proton transfer in the transition state are important aspects of both the uncatalyzed and the autocatalytic routes to amidine **3**. Detailed understanding of these factors played an essential role during the development of a robust commercial manufacturing process for saxagliptin.

EXPERIMENTAL SECTION

(1*aS*,4*S*,6*aR*,7*aS*)-4-((1*R*,3*R*,5*R*,7*S*)-3-Hydroxyadamantan-1-yl)-6-iminohexahydro-1*H*-cyclopropa[4,5]pyrrolo[1,2-*a*]pyrazin-3(1*aH*)-one (**3**). A mixture of saxagliptin (**1**, 66.6 g, 200 mmol) and *n*-BuOH (250 mL) was stirred at 90 °C. Then, *n*-BuOAc (350 mL) was added to the resulting suspension, and the mixture was heated to reflux until a pale yellow solution was obtained. To remove water from the mixture, 120 mL of *n*-BuOH/*n*-BuOAc azeotrope were collected and discarded. After 3 h at reflux, the amidine **3** started to precipitate out. The suspension was refluxed for 5 h, cooled to rt, and stirred for 16 h at rt. The mixture was filtered, and the filter cake was washed with EtOAc (200 mL) and dried with suction. The crude material (44.6 g) was dissolved in *i*-PrOH (900 mL) at reflux, and the solution was polish filtered hot. The solution was concentrated at atmospheric pressure to ca. 300 mL to afford a suspension that was cooled to rt and filtered with suction. The solid was washed with *i*-PrOH (150 mL) and dried under vacuum (~3 mmHg, 55–60 °C) to constant weight for 1 h to yield the desired amidine **3** as white crystals (24.2 g, 38.4%): mp > 209.7 °C; ¹H NMR (300 MHz, MeOH-*d*₄) δ

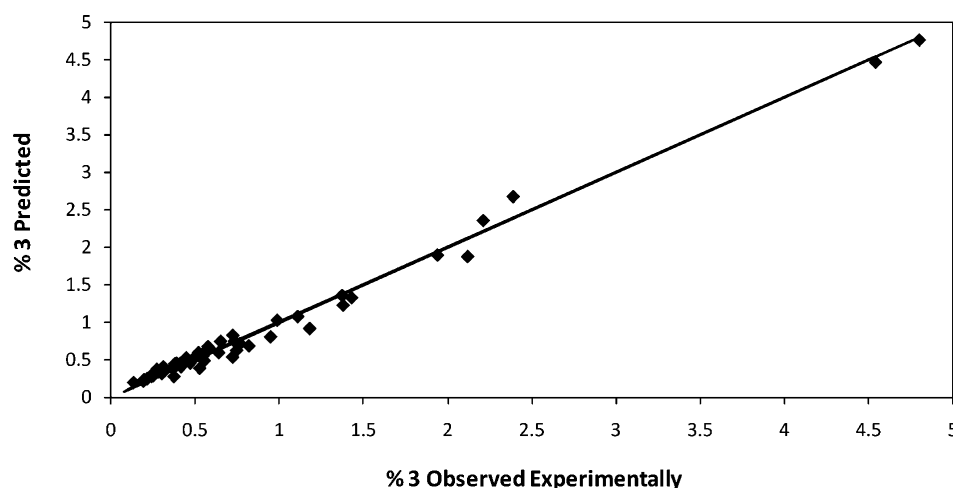


Figure 5. Parity plot of predicted versus experimentally observed data.

0.77 (m, 1H), 0.83 (dd, $J = 10.5, 6.0$ Hz, 1H), 1.47–1.70 (m, 11H), 2.03 (m, 1H), 2.16 (br s, 2H), 2.52 (m, 1H), 3.56 (br s, 1H), 3.89 (br t, $J = 7.5$ Hz, 1H), 4.08 (ddd, $J = 6.0, 6.0, 3.0$ Hz, 1H); ^{13}C NMR (75 MHz, CDCl_3) δ 7.9, 12.1, 31.8, 32.3, 35.2, 36.5, 39.1, 45.0, 45.2, 47.4, 53.7, 69.2, 70.9, 160.9, 168.9; HRMS calculated for $\text{C}_{18}\text{H}_{26}\text{N}_3\text{O}_2$ [$\text{M} + \text{H}^+$] 316.2025, found 316.2029.

Isolation of (1aS,4S,6aS,7aS)-4-[(1R,3R,5R,7S)-3-Hydroxyadamantan-1-yl]-6-imino-hexa-hydro-1H-cyclopropa[4,5]pyrrolo[1,2-a]pyrazin-3(1aH)-one (2). A series of saxagliptin (1) tablets stressed at 50 °C in a stability study were crushed and extracted with 0.1 N HCl. The resulting extract was lyophilized, and amidine 9 was isolated using semipreparative HPLC: ^1H NMR (400 MHz, $\text{DMSO}-d_6$) δ 0.42 (ddd, $J = 5.0, 5.0, 2.5$ Hz, 1H), 1.06 (ddd, $J = 8.3, 5.0, 5.0$ Hz, 1H), 1.45–1.70 (m, 10H), 1.60–2.00 (m, 2H), 1.77 (m, 1H), 1.96 (ddd, $J = 13.3, 8.7, 2.0$ Hz, 1H), 2.12 (br s, 2H), 2.76 (ddd, $J = 13.3, 7.9, 7.9$ Hz, 1H), 3.35 (m, 1H), 3.74 (br s, 1H), 5.20 (t, $J = 7.9$ Hz, 1H), 8.62 (s, 1H), 9.18 (s, 1H), 9.38 (s, 1H); ^{13}C NMR (100 MHz, CDCl_3) δ 14.8, 21.0, 31.2, 36.3, 60.7, 61.3, 66.4, 163.5, 164.6; HRMS calculated for $\text{C}_{18}\text{H}_{26}\text{N}_3\text{O}_2$ [$\text{M} + \text{H}^+$] 316.2025, found 316.2035.

(1aS,4R,6aR,7aS)-4-[(1S,3S,5R)-3-Hydroxyadamantan-1-yl]-tetrahydro-1H-cyclopropa-[4,5]pyrrolo[1,2-a]pyrazine-3,6-(1aH,6aH)-dione (4). A suspension of amidine 3 (12.5 g, 40 mmol) in water (125 mL) was stirred at 85 °C in a flask equipped with a bubbler to allow the escape of ammonia formed by the reaction. After heating the mixture for 1 h, additional water (50 mL) was added. The suspension was heated for 18 h, at which time LC–MS analysis indicated that the mixture contained approximately equal proportions of amidine 3 and diketopiperazine 4. The suspension was then cooled to rt and filtered. The filtrate containing 4 was evaporated, and the residue was azeotroped with *i*-PrOH (1 L). The residue was dissolved in MeOH (300 mL) and decolorized with 3 g of charcoal. The resulting suspension was filtered through Celite, and the solvent was evaporated at reduced pressure to give an off-white solid that was then dissolved in *i*-PrOH (350 mL). The solvent was switched at normal pressure from *i*-PrOH to EtOAc, and a total of 2 L of distillate was collected. Diketopiperazine 4 precipitated during the distillation, which was stopped when the final volume of the suspension reached ca. 300 mL. The mixture was cooled to rt, and the solid was filtered and washed with EtOAc (50 mL). The collected white solid was dried under vacuum (2 mmHg, 60 °C) to constant weight for 1 h to afford the desired diketopiperazine 4 (6.2 g, 50%): mp 260–261 °C; ^1H NMR (300 MHz, $\text{MeOH}-d_4$) δ 0.79 (m, 1H), 0.84 (dd, $J = 9.0, 6.0$ Hz, 1H), 1.45–1.72 (m, 11H), 2.16 (m, 1H), 2.21 (br s, 2H), 2.42 (dd, $J = 13.5, 7.5$ Hz, 1H), 3.48 (br s, 1H), 4.01 (m, 2H); ^{13}C NMR (75 MHz, CDCl_3) δ 8.4, 12.6, 31.6, 36.1, 38.6, 44.2, 45.0, 47.0, 55.6, 67.2, 69.0, 165.4, 171.7; HRMS calculated for $\text{C}_{18}\text{H}_{25}\text{N}_2\text{O}_3$ [$\text{M} + \text{H}^+$] 317.1865, found 317.1865.

■ ASSOCIATED CONTENT

📄 Supporting Information

General methods, rate data, copies of NMR spectra, and molecular modeling coordinates. This material is available free of charge via the Internet at <http://pubs.acs.org>.

■ AUTHOR INFORMATION

✉ Corresponding Author

*E-mail: scott.jones@bms.com.

📍 Present Address

[†]Department of Bioengineering, Stanford University, 318 Campus Drive, Stanford, California 94305, United States.

■ ACKNOWLEDGMENTS

The authors would like to thank Venkatramana Rao for contributing the deuterium exchange work referenced here and for useful discussions during this research. The authors would also like to thank Yande Wang for the isolation and characterization of amidine 2 during drug product stability studies.

■ REFERENCES

- (1) FDA News Release: FDA Approves New Drug Treatment for Type 2 Diabetes. <http://www.fda.gov/NewsEvents/Newsroom/PressAnnouncements/ucm174780.htm> (July 31, 2009).
- (2) Havale, S. H.; Manojit, P. *Bioorg. Med. Chem.* **2009**, *17*, 1783.
- (3) Magnin, D. R.; Robl, J. A.; Sulsky, R. B.; Augeri, D. J.; Huang, Y.; Simpkins, L. M.; Taunk, P. C.; Betebenner, D. A.; Robertson, J. G.; Abboa-Offei, B. E.; Wang, A.; Cap, M.; Xin, L.; Tao, L.; Sitkoff, D. F.; Malley, M. F.; Gougoutas, J. Z.; Khanna, A.; Huang, Q.; Han, S.-P.; Parker, R. A.; Hamann, L. G. *J. Med. Chem.* **2004**, *47*, 2587.
- (4) Fura, A.; Khanna, A.; Vyas, V.; Koplowitz, B.; Chang, S.-Y.; Caporuscio, C.; Boulton, D. W.; Christopher, L. J.; Chadwick, K. D.; Hamann, L. G.; Humphreys, W. G.; Kirby, M. *Drug Metab. Dispos.* **2009**, *37*, 1164.
- (5) Savage, S. A.; Jones, G. S.; Kolotuchin, S.; Ramrattan, S. A.; Vu, T.; Waltermire, R. E. *Org. Process Res. Dev.* **2009**, *13*, 1169.
- (6) Amidine 2 was observed during solid state stability studies of (1) amorphous saxagliptin (1) as well as (2) saxagliptin tablets.
- (7) A 2:1 solution of saxagliptin (1) and its epimer was prepared in isopropanol and subsequently monitored for conversion to amidine 3. After approximately 30% conversion to amidine 3, saxagliptin (1) and its epimer remained at a 2:1 ratio, and both had converted exclusively to amidine 3 at the same rate. This observation, together with the fact that none of amidine 2 is observed when saxagliptin (1) cyclizes in

solution, refutes the possibility of slow epimerization of saxagliptin (1) followed by rapid cyclization.

(8) Marcus, Y. *The Properties of Solvents*; John Wiley & Sons: Chichester, U. K., 1998; Wiley Series in Solution Chemistry Vol. 4.

(9) For a detailed description of the technique and the application of the Gross-Butler equation, see: Venkatasubban, K. S.; Schowen, R. L. *Crit. Rev. Biochem.* **1984**, *17*, 1.

(10) For simplicity, we assume that the fractionation factors for exchangeable protons in the reactants, Φ_i^R , are unity. Considering that the primary amine **1** and isopropyl alcohol are involved in the reaction, this assumption simply means that the distribution of deuterium in these species is equal to the distribution of deuterium in the bulk solvent, isopropyl alcohol. For alcohols and amines, the assumption that $\Phi_i^R \sim 1$ is generally considered valid as these protons are readily exchangeable.¹¹ With this assumption, the denominator of eq 1 is unity.

(11) Schowen, K. B. J. In *Transition States of Biochemical Processes*; Gandour, R. D., Schowen, R. L., Eds.; Plenum Press: New York, 1978.

(12) The calculations incorporate thermal corrections to Gibbs free energies, polarized continuum model (PCM) adjustments for *i*-PrOH as the bulk solvent, and corrections to basis set superposition errors (BSSE) using the counterpoise method as implemented in Gaussian'09. See the Supporting Information for details and references.

(13) For a discussion on the limitations of replacing discrete solvation by a continuum in H-bonded systems, see: *Continuum Solvation Models in Chemical Physics: From Theory to Applications*; Tomasi, J., Mennucci, B., Cammi, R., Eds.; Wiley: Chichester, U. K., 2007.

(14) During the development of the saxagliptin manufacturing process, it was observed that the rate of cyclization increases monotonically with pH.

(15) Swain, C. G.; Brown, J. F. Jr. *J. Am. Chem. Soc.* **1952**, *74*, 2538.

(16) Field, M. J.; Hillier, I. H. *J. Chem. Soc., Perkin Trans. 2* **1987**, 617.

(17) (a) Chen, Y.; Gai, F.; Petrich, J. W. *J. Am. Chem. Soc.* **1993**, *115*, 10158. (b) Boyle, P. H.; Convery, M. A.; Davis, A. P.; Hosken, G. D.; Murray, B. A. *J. Chem. Soc. Chem. Commun.* **1992**, 239.

(18) Acidity values in aqueous solution: Bordwell, F. G. *Acc. Chem. Res.* **1988**, *21*, 456.

(19) Arrhenius E_a and Eyring ΔG_{298}^\ddagger values were calculated from plots of $\ln(k)$ and $\ln(k/T)$ as a function of $1/T$, respectively.

(20) Within the range of isopropanol concentrations germane to the saxagliptin process, the rate is first order in isopropanol. For broader ranges, the rate may demonstrate saturation kinetics.